

SCIENTIFIC REPORTS



OPEN

SHP2 Regulates the Osteogenic Fate of Growth Plate Hypertrophic Chondrocytes

Lijun Wang¹, Jiahui Huang¹, Douglas C. Moore¹, Chunlin Zuo^{1,8}, Qian Wu², Liqin Xie³, Klaus von der Mark⁴, Xin Yuan⁵, Di Chen⁶, Matthew L. Warman⁷, Michael G. Ehrlich¹ & Wentian Yang¹

Transdifferentiation of hypertrophic chondrocytes into bone-forming osteoblasts has been reported, yet the underlying molecular mechanism remains incompletely understood. SHP2 is an ubiquitously expressed cytoplasmic protein tyrosine phosphatase. SHP2 loss-of-function mutations in chondroid cells are linked to metachondromatosis in humans and mice, suggesting a crucial role for SHP2 in the skeleton. However, the specific role of SHP2 in skeletal cells has not been elucidated. To approach this question, we ablated SHP2 in collagen 2 α 1(Col2 α 1)-Cre- and collagen 10 α 1(Col10 α 1)-Cre-expressing cells, predominantly proliferating and hypertrophic chondrocytes, using “Cre-loxP”-mediated gene excision. Mice lacking SHP2 in Col2 α 1-Cre-expressing cells die at mid-gestation. Postnatal SHP2 ablation in the same cell population caused dwarfism, chondrodysplasia and exostoses. In contrast, mice in which SHP2 was ablated in the Col10 α 1-Cre-expressing cells appeared normal but were osteopenic. Further mechanistic studies revealed that SHP2 exerted its influence partly by regulating the abundance of SOX9 in chondrocytes. Elevated and sustained SOX9 in SHP2-deficient hypertrophic chondrocytes impaired their differentiation to osteoblasts and impaired endochondral ossification. Our study uncovered an important role of SHP2 in bone development and cartilage homeostasis by influencing the osteogenic differentiation of hypertrophic chondrocytes and provided insight into the pathogenesis and potential treatment of skeletal diseases, such as osteopenia and osteoporosis.

Skeletal development occurs through two distinct processes: intramembranous ossification, which generates craniofacial bones and the lateral part of clavicles, and endochondral ossification, which produces the long bones of the limbs, the base of the skull, the vertebrae, the ribs and medial part of the clavicles¹. Beginning with the condensation of undifferentiated mesenchymal cells, intramembranous ossification forms flat bones in mesenchymal tissue without a cartilaginous anlagen². By contrast, during endochondral ossification, cells within the center of the condensation differentiate into chondrocytes that secrete extracellular matrix (ECM) rich in aggrecan and collagen type II (COL2 α 1)^{3,4}. As endochondral ossification progresses, cells in the center of the condensation exit the cell cycle, undergo hypertrophic differentiation, and begin to produce ECM rich in collagen type X (COL10 α 1), which is calcified during skeletal development⁵. Terminally differentiated hypertrophic chondrocytes are ultimately removed from the cartilage template as the mineralized cartilage matrix is replaced by bone. It is well established that many of the hypertrophic chondrocytes are removed via programmed (apoptotic or autophagic) cell death^{6,7}. However, there is increasing evidence that a substantial fraction of the hypertrophic chondrocytes in the growth plate transdifferentiate into osteoblasts that persist to produce trabecular bone and maintain mineral homeostasis^{8–10}.

¹Department of Orthopaedic Surgery, Brown University Alpert Medical School, Providence, RI, 02903, USA.

²Department of Pathology and Laboratory Medicine, University of Connecticut Health Center, Farmington, CT, 06030, USA.

³Regeneron Pharmaceuticals, Tarrytown, NY, 10591, USA. ⁴Department of Experimental Medicine, University of Erlangen-Nürnberg, Gluckstrasse 6, 91054, Erlangen, Germany.

⁵Department of Medicine, Beth Israel Deaconess Medical Center and Harvard Medical School, Boston, MA, 02115, USA. ⁶Department of Biochemistry, Rush University, 600 S. Paulina St., Chicago, IL, 60612, USA.

⁷Orthopaedic Research Laboratories and Howard Hughes Medical Institute, Boston Children’s Hospital and Harvard Medical School, Boston, MA, 02115, USA. ⁸Present address: Department of Endocrinology, the First Affiliated Hospital of Anhui Medical University, Hefei, 230022, P.R. China.

Correspondence and requests for materials should be addressed to W.Y. (email: wyang@lifespan.org)

The formation of the cartilage anlage, its subsequent differentiation into mature chondrocytes, and the ultimate transdifferentiation of hypertrophic chondrocytes into functioning osteoblasts all depend on signals evoked by growth factors and other regulatory peptides^{11,12}, though cell-cell, and cell-matrix interactions are also important^{13,14}. Besides producing ECM proteins, terminally differentiated hypertrophic chondrocytes release matrix metalloproteases, such as MMP13, MMP9, and cathepsins^{15–17}, and growth factors (e.g. VEGF, IGF1, RANKL, and FGFs), which influence matrix remodeling, osteoclast precursor recruitment and subsequent osteoclastogenesis at the chondro-osseous front, respectively^{18,19}. The coordinated coupling of these events is critical for skeletal development and longitudinal bone growth. Although the exact molecular signals controlling these processes remain incompletely understood, the coordinated activation of sequential signaling pathways involving FGF, WNT/ β -CATENIN, hedgehog, and BMP have been shown to be crucial^{20–27}. Understanding how these signaling pathways are regulated will provide insight into skeletal development and the treatment of disease.

SHP2, encoded by *PTPN11*, is a widely expressed SH2 domain-containing non-receptor protein tyrosine phosphatase. Its orthologs are shared by nearly all vertebrates, functioning to regulate the viability, proliferation, differentiation, and migration of a wide variety of cells^{28,29}. Accumulating evidence suggests a crucial role for SHP2 in skeletal development and maintenance. In humans, SHP2 gain-of-function (GOF) mutations cause Noonan Syndrome (NS), whose skeletal manifestations include short stature, scoliosis, pectus malformation and craniofacial abnormalities (macrocephaly, oral malformation and hypertelorism)^{30,31}. Mice bearing SHP2 GOF mutations are small, and have increased skull length and hypertelorism³². Hyperactivation of ERK1/2 signaling reportedly causes these developmental abnormalities, and inhibition of ERK1/2 can rescue the skull defects in mice with NS^{32–34}. Conversely, SHP2 loss-of-function (LOF) mutations have been linked to the benign cartilage tumor syndrome metachondromatosis, in both humans and mice^{35–38}. Thus, alterations in the expression of SHP2 can be associated with both osteogenic and chondrogenic phenotypes. The specific role of SHP2 in skeletal development and disease is an important question that has yet to be explored.

The SOX9 and WNT/ β -CATENIN signaling pathways are important regulators of chondrogenesis and osteoblastogenesis, respectively³⁹. SOX9, a member of the high-mobility group (HMG) DNA-binding proteins, is considered a master chondrogenic transcription factor. SOX9 expression commences in mesenchymal precursors and persists through chondrocyte hypertrophy^{40–42}. SOX9 promotes the expression of critical chondrocytic genes, including *Col2 α 1*, *Col10 α 1*, *Matn3* and *Acan*^{41,43}, and inhibits the terminal differentiation and *Vegf α* expression of hypertrophic chondrocytes^{42,44}. Downregulation of SOX9 in the hypertrophic layer of growth plate cartilage disinhibits vascular invasion and endochondral ossification⁴². β -CATENIN and RUNX2, on the other hand, are crucial for osteoblastogenesis and ossification^{45–48}. Removal of β -CATENIN from hypertrophic chondrocytes impairs their osteogenic differentiation and trabecular bone formation, while sustained β -CATENIN activation leads to enhanced bone mineralization⁴⁹. This suggests that β -CATENIN signaling is crucial for the transdifferentiation of hypertrophic chondrocytes.

SHP2 has been implicated in the regulation of SOX9^{50,51}, which is an antagonist of β -CATENIN^{45,52}. However, it is unknown whether the abundance and transcriptional activity of SOX9 and β -CATENIN in hypertrophic chondrocytes, and whether the osteogenic differentiation of hypertrophic chondrocytes, are modulated by SHP2. To begin addressing these questions, we generated chondrocyte-stage-specific SHP2 deficient mice. Characterization of the skeletal phenotype of mice lacking SHP2 in COL2 α 1- and COL10 α 1-expressing cells led to the discovery of SHP2 as an important regulator of chondrocyte proliferation, maturation, and differentiation to bone forming osteoblasts.

Results

SHP2 deletion in COL2 α 1- but not COL10 α 1-expressing cells causes dwarfism, exostoses, and chondrodysplasia. A “Cre-loxP”-mediated gene deletion approach was used to study the function of SHP2 in cartilage and circumvent the embryonic lethality of global SHP2 deletion (Fig. S1)^{53,54}. Control and SHP2 knockout mice were generated by crossing homozygous *Ptpn11* floxed (*Ptpn11^{fl/fl}*) mice³⁶ with SHP2 heterozygous (*Ptpn11^{fl/+}*) mice carrying *Col2 α 1* or *Col10 α 1* promoter-driven Cre recombinase^{55,56} (Fig. S1A). Breeders for the SHP2 ablation in chondrocytes were generated by crossing mice bearing a single *Ptpn11* floxed allele (*Ptpn11^{fl/+}*) to transgenic mice in which Cre expression is under the control of *Col2 α 1*^{55,57} or *Col10 α 1* promoter⁵⁶. Deleting SHP2 in proliferating chondrocytes required tamoxifen-inducible *Tg(Col2 α 1-CreERT2)*⁵⁵, since SHP2 deletion via *Tg(COL2 α 1-Cre)*⁵⁷ resulted in intrauterine death by day E11.5 (Fig. S1C,D). The final breeding strategy yielded *Ptpn11^{fl/+};Tg(Col2 α 1-CreERT2)*, *Ptpn11^{fl/fl};Tg(Col2 α 1-CreERT2)*, *Ptpn11^{fl/+};Tg(Col10 α 1-Cre)*, and *Ptpn11^{fl/fl};Tg(Col10 α 1-Cre)* compound mice, abbreviated as SHP2_{Col2 α 1ER}CTR, SHP2_{Col2 α 1ER}KO, SHP2_{Col10 α 1}CTR, and SHP2_{Col10 α 1}KO, respectively (Fig. S1B). *Tg(Col2 α 1-CreERT2)* and *Tg(Col10 α 1-Cre)* mice express a functional Cre in COL2 α 1- and COL10 α 1-expressing chondrocytes as revealed by *Rosa26^{lacZ}* (*R26^{lacZ}*) reporter⁵⁸ (Fig. S2A–C).

Age- and sex-matched SHP2_{Col2 α 1ER}CTR and SHP2_{Col2 α 1ER}KO mice received three doses of tamoxifen (TM) at the end of postnatal week 2 and cohorts of animals from SHP2_{Col2 α 1ER}CTR, SHP2_{Col2 α 1ER}KO, SHP2_{Col10 α 1}CTR and SHP2_{Col10 α 1}KO strains were euthanized at weeks 6, 8 and 10 for skeletal development evaluation. By 8 weeks SHP2_{Col2 α 1ER}KO mice were significantly smaller (–17%) than the corresponding SHP2_{Col2 α 1ER}CTR mice (13.63 \pm 0.48 cm vs. 16.38 \pm 0.75 cm, n = 4) (Fig. 1Ai,ii; Fig. S3A). Other features of the skeletal phenotype in adult SHP2_{Col2 α 1ER}KO mice included scoliosis, small rib cages, and multiple joint dysplasias affecting the phalanges, metatarsals, knees, hips, vertebrae and chondrocostal junctions (Fig. 1Ai–x, Bi–iv). Micro-CT (μ -CT) and x-ray imaging revealed the existence of exostoses at the knees and hips, deformed pelvises, shallow acetabulums and misshapen femoral heads and greater trochanters (Fig. 1Bi–iv and Fig. 2D). Of note, the bone mineral density in the SHP2_{Col2 α 1ER}KO mice was reduced compared to sex- and age-matched SHP2_{Col2 α 1ER}CTR mice (Fig. 1Aix,x), and the growth plates in the caudal vertebrae (Fig. 1Av,vi, arrows) and other tubular bones of the SHP2_{Col2 α 1ER}KO mice were much wider than those of the SHP2_{Col2 α 1ER}CTR mice. Similar morphological analysis was performed

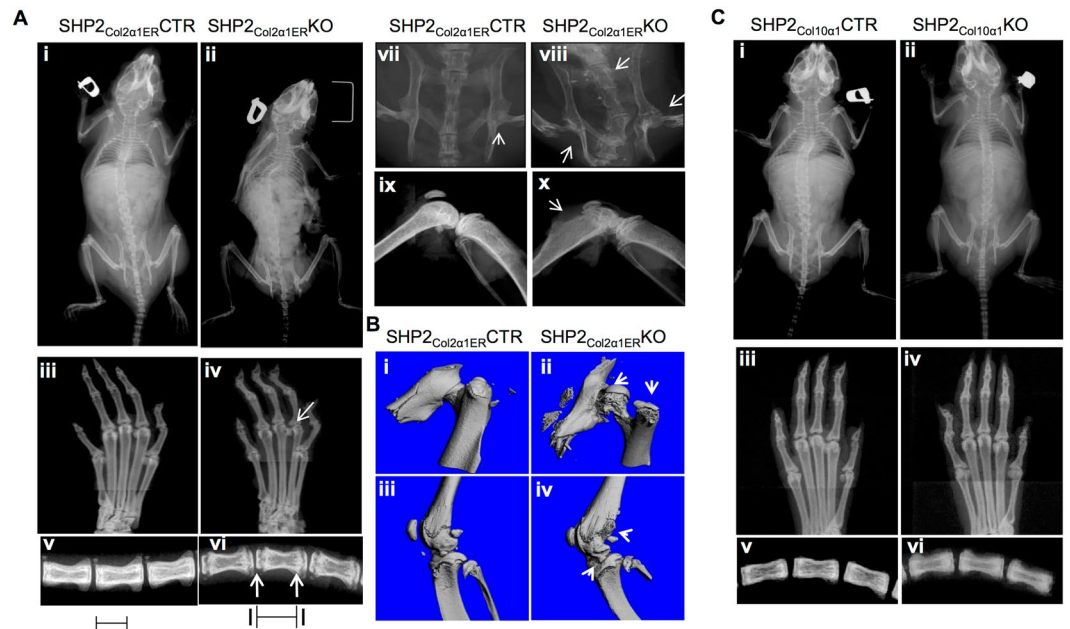


Figure 1. Mice with SHP2 deletion in COL2 α 1- and COL10 α 1-expressing cells have osteopenia, and SHP2 deletion in COL2 α 1- but not COL10 α 1-expressing chondrocytes causes dwarfism, exostoses, and multiple joint dysplasia. (A) X-ray images demonstrate dwarfism and scoliosis (i, ii), and chondrodysplasia of the metatarsophalangeal joints (iii, iv), caudal vertebrae (v, vi), hip (vii, viii) and knee joints (ix, x) in 8-week-old SHP2^{Col2 α 1ER}KO mice, compared to age and sex-matched SHP2^{Col2 α 1ER}CTR mice. Note that SHP2^{Col2 α 1ER}KO mice exhibited slightly reduced bone mineral density, exostoses, and a broadened growth plate cartilage in the caudal vertebrae (v, vi, bars and arrows). (B) Representative μ -CT images show the shallow acetabular sockets, misshapen femoral heads and greater trochanters (i, ii) and exostoses (iii, iv) in SHP2^{Col2 α 1ER}KO mice, compared to SHP2^{Col2 α 1ER}CTR mice. (C) X-ray images demonstrate comparable morphology in 10-week-old SHP2^{Col10 α 1}CTR and SHP2^{Col10 α 1}KO mice. Note the slight decrease in bone mineral density in SHP2^{Col10 α 1}KO mice compared to SHP2^{Col10 α 1}CTR controls (n = 4).

on the SHP2^{Col10 α 1}KO and SHP2^{Col10 α 1}CTR mice. In contrast to the SHP2^{Col2 α 1ER}KO mice, there were no gross skeletal defects in the SHP2^{Col10 α 1}KO mice through 10 weeks of age. However, the SHP2^{Col10 α 1}KO mice did exhibit the same apparent reduction in bone mineralization compared to corresponding sex- and age-matched SHP2^{Col2 α 1ER}CTR mice (Fig. S3B).

Taken together, these data suggest that functional SHP2 is crucial for normal cartilage development and bone mineralization in COL2 α 1-expressing chondrocytes, but that it only influences bone mineral homeostasis in COL10 α 1-expressing chondrocytes.

Cartilage and bone development require SHP2. Having established the importance of SHP2 in both cartilage and bone development, we sought to explore the cellular mechanisms by which SHP2 regulates skeletogenesis. To start, knee joints from TM-treated 6- and 8-week-old SHP2^{Col2 α 1ER}CTR and SHP2^{Col2 α 1ER}KO mice were harvested and examined histologically. By 6 weeks of age the SHP2^{Col2 α 1ER}CTR mice had well-organized growth plates and articular cartilage stained strongly positive for proteoglycan (Fig. 2Ai,iii,v). In contrast, the columnar structure of the growth plate cartilage in the SHP2^{Col2 α 1ER}KO mice was dysregulated, featuring significantly expanded proliferating and hypertrophic zones (Fig. 2Aii,iv; Fig. S4A). Similar morphologic changes were observed in SHP2^{Col2 α 1ER}KO mice bearing a R26^{mTg} reporter (Fig. S4B). These drastic changes in the growth plate cartilage of SHP2^{Col2 α 1ER}KO mice were not observed in SHP2^{Col10 α 1}KO mice, which had normal-appearing cartilage with the exception of a slight increase in height of the hypertrophic layer of chondrocytes at 8 weeks (Fig. 2B). Surprisingly, the articular cartilage in the knee joints in the SHP2^{Col2 α 1ER}KO, SHP2^{Col10 α 1}KO, and littermate control mice were comparable at 6 and 8 weeks of age. (Fig. 2Av,vi; Bv,vi and Fig. S4Biii,iv), though the adult SHP2^{Col2 α 1ER}KO mice developed exostoses and enchondromas at the metaphyseal regions of the long bones and vertebrae (Fig. 2C and D).

To investigate whether SHP2 was required for cell proliferation in COL2 α 1-expressing physal cartilage cells as it is in many other cell types^{28,29}, pregnant females that had received 2 doses of TM injections at embryonic (E) day 13.5 and E15.5 were administered one dose of 5-ethynyl-2-deoxyuridine (EdU) at E16.5, and sacrificed at E17.5 to collect embryos. EdU staining of tibia frozen sections from these mice revealed an increased number of EdU+ cells in SHP2^{Col2 α 1ER}KO mice, compared to SHP2^{Col2 α 1ER}CTR mice, indicating that SHP2 deletion in COL2 α 1-expressing cells promoted EdU uptake and that under normal condition SHP2 functions as a negative regulator of chondrocyte proliferation (Fig. S4C).

Given the apparent reduction in x-ray bone mineral density in the COL2 α 1+ and COL10 α 1+ cell-specific SHP2 knockout mice, we performed histomorphometric analysis on von Kossa-stained femoral sections from

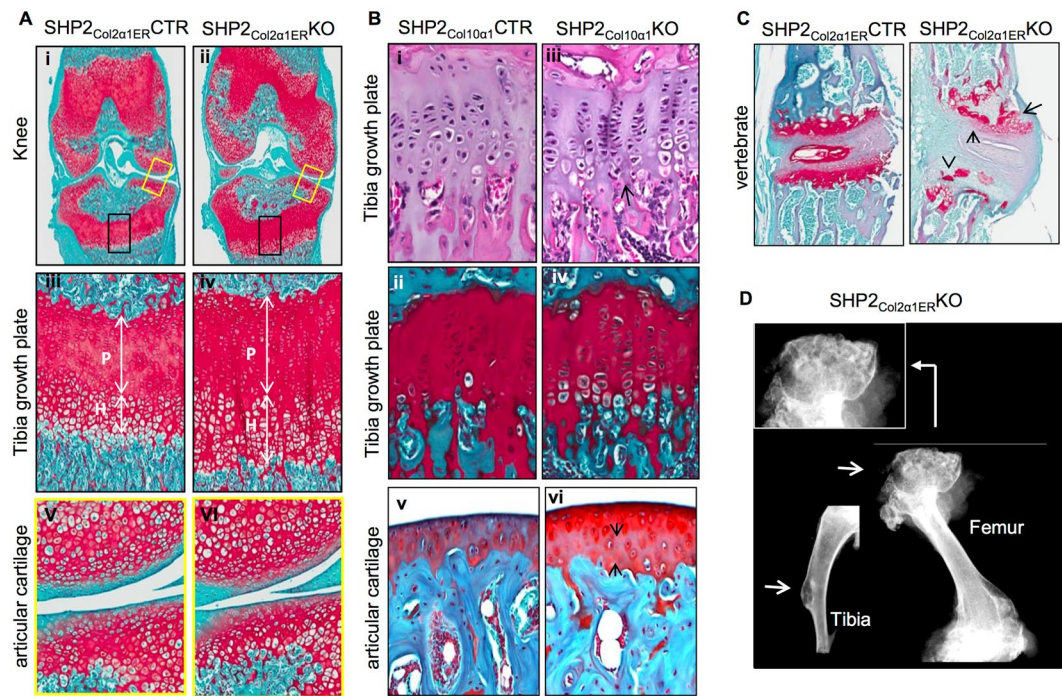


Figure 2. SHP2 modulates the proliferation and hypertrophic differentiation of growth plate chondrocytes. (A) Representative images of mouse knee joint coronal sections stained with Safranin O/fast green demonstrating broad, disorganized growth plate cartilage, affecting both proliferating (P) and hypertrophic (H) chondrocytes (double arrow lines) in 6-week-old SHP2^{Col2a1ER}KO mice compared to SHP2^{Col2a1ER}CTR mice. SHP2^{Col2a1ER}KO and SHP2^{Col2a1ER}CTR mice received TM injection at the end of week 2. Note that the articular cartilage in the SHP2^{Col2a1ER}CTR and SHP2^{Col2a1ER}KO mice is grossly similar at this age. Images iii to vi are enlarged views of the color-bounded areas in images i and ii. $n = 4$. (B) Images of 8-week-old mouse proximal tibia sections stained with H&E, Safranin O/fast green demonstrating comparable growth plate and articular cartilage morphology in SHP2^{Col10a1}CTR and SHP2^{Col10a1}KO mice ($n = 5$). (C) Images of vertebral sections stained with Safranin O demonstrate enchondromas (arrows) developed in 10-week-old SHP2^{Col2a1ER}KO mice (SHP2^{Col2a1ER}CTR served as controls). Both mice received TM injection at the end of week 2 ($n = 5$). (D) Representative x-ray images of femur and tibia harvested from 10-week-old SHP2^{Col2a1ER}KO mice demonstrating exostoses in the proximal femur and an enchondroma in the tibia (arrow) ($n = 5$).

10-week-old SHP2^{Col2a1ER}KO and SHP2^{Col10a1}KO mice. SHP2 deletion in both knockout strains was associated with a significant reduction of calcified trabecular bone compared to age- and sex-matched controls (Fig. 3A). These observations were generally supported by microcomputed tomographic analysis (μ CT), which revealed significant decreases in volumetric density (bone volume/total volume or BV/TV) and trabecular thickness (Tb. th.) in SHP2^{Col2a1ER}KO and SHP2^{Col10a1}KO mice compared to their corresponding controls (SHP2^{Col2a1ER}CTR and SHP2^{Col10a1}CTR, respectively) (Fig. 3B). The structure model index (SMI) increased in the SHP2^{Col2a1ER}KO mice. Trabecular number (Tb.N), space (Tb.S), and connectivity density (conn dens) were not significantly affected at this time point. Collectively, the histology, cell proliferation, and morphometric results demonstrate that SHP2 has a developmental stage-specific role in chondrogenesis and that SHP2 regulates bone mineral homeostasis in SHP2^{Col2a1ER}KO and SHP2^{Col10a1}KO through its effect on chondroid cells.

SHP2 regulates the osteogenic differentiation of growth plate hypertrophic chondrocytes. The transdifferentiation of COL10 α 1+ growth plate chondrocytes into osteoblasts and osteocytes has been reported^{8–10} and has now been established as a process crucial for endochondral ossification and mineral homeostasis^{49,59}. Our observation that mineralization was reduced in mice lacking SHP2 in Col10 α 1-expressing chondrocytes (radiographically and via μ CT) prompted us to investigate whether SHP2 might influence the differentiation of hypertrophic chondrocytes into osteoblasts. To start, we performed fluorescent reporter-based cell lineage tracing using SHP2^{Col10a1}CTR;R26^{ZsG} and SHP2^{Col10a1}KO;R26^{ZsG} mice crossed to *Sp7^{mCherry}* reporter mice⁶⁰ (SHP2^{Col10a1}CTR;R26^{ZsG};Sp7^{mCherry} and SHP2^{Col10a1}KO;R26^{ZsG};Sp7^{mCherry}, respectively). In these mice COL10 α 1(R26^{ZsG})-positive cells fluoresce green, OSTERIX (SP7^{mCherry})-positive cells fluoresce red, and COL10 α 1(R26^{ZsG})/OSTERIX (SP7^{mCherry})-double positive cells fluoresce yellow. Yellow fluorescence identifies cells of COL10 α 1-expressing origin that subsequently began expressing OSTERIX, and thus were capable of participating in osteoblastogenesis and endochondral ossification.

Frozen sections from P0.5 day-old pups revealed COL10 α 1+/OSTERIX+ double positive (yellow) cells in the developing metaphyseal cancellous bone of both SHP2^{Col10a1}CTR;R26^{ZsG};Sp7^{mCherry} and SHP2^{Col10a1}KO;R26^{ZsG};Sp7^{mCherry} mice, but not in the growth plate and articular cartilage. Importantly, there were

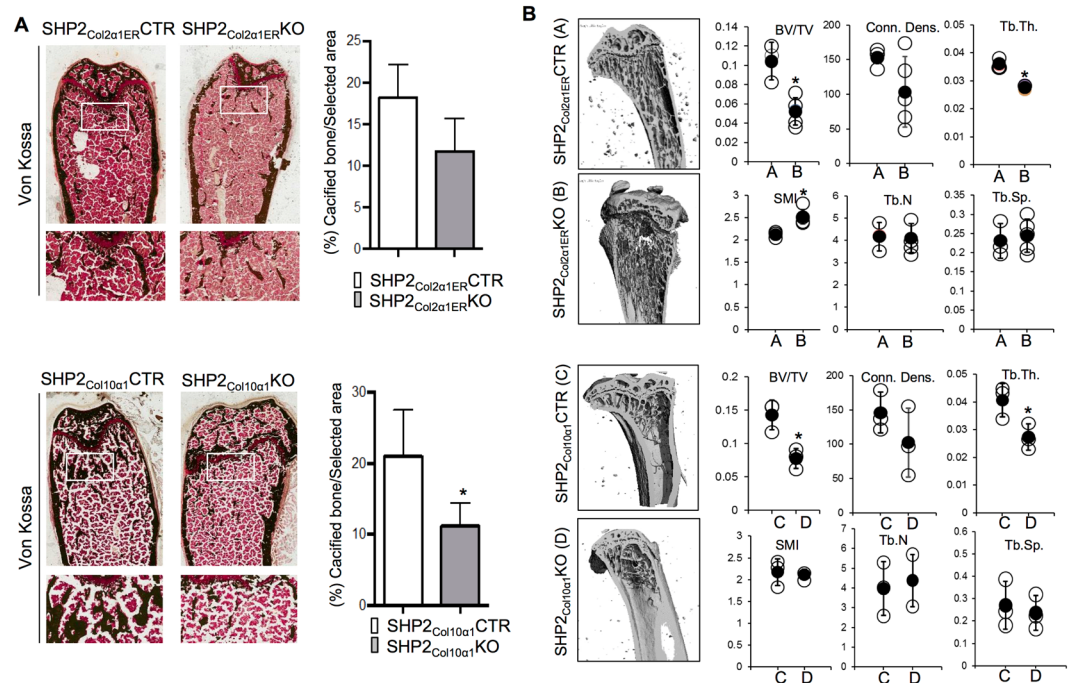


Figure 3. SHP2 deletion in COL2 α 1- and COL10 α 1-expressing cells compromised endochondral ossification. **(A)** Representative images of von Kossa/Fast red stained mouse femoral sections demonstrating a reduction of cancellous bones in 10-week-old SHP2_{Col2 α 1ER}KO and SHP2_{Col10 α 1}KO mice, compared to SHP2_{Col2 α 1ER}CTR and SHP2_{Col10 α 1}CTR mice. Mineralized bone was segmented from an 800 μ m \times 1200 μ m rectangular region interested below the growth plate cartilage and quantified using NIH ImageJ software (n = 4, *p < 0.05, Student's t test). **(B)** μ -CT analysis of proximal tibia morphology demonstrating reduced BV/TV and Tb.Th in 10-week-old SHP2_{Col2 α 1ER}KO and SHP2_{Col10 α 1}KO mice, compared to SHP2_{Col2 α 1ER}CTR and SHP2_{Col10 α 1}CTR controls (n = 4, *p < 0.05, Student's t test). BV/TV: bone volume/total volume; Tb.Th: trabeculae thickness; Tb.N: trabeculae number; Tb.Sp: trabecule space; Conn.Dens: connectivity density; SMI: Structure model index.

fewer, sparsely scattered COL10 α 1+/OSTERIX+ double positive cells in the SHP2_{Col10 α 1}KO;R26^{ZsG};Sp7^{mCherry} mice compared to the SHP2_{Col10 α 1}CTR;R26^{ZsG};Sp7^{mCherry} controls (mean \pm stdv of percentage: 56.75 \pm 10.58 vs. 43.17 \pm 13.05. *p < 0.05, Student's t test) (Fig. 4 A–C). Similar results were seen in P9.5 SHP2_{Col10 α 1}CTR;R26^{mTG} and SHP2_{Col10 α 1}KO;R26^{mTG} newborns. Intriguingly, GFP+ cells accumulated in the hypertrophic layer of growth plate cartilage in SHP2_{Col10 α 1}KO;R26^{mTG} mice (Fig. S5). Collectively, our cell lineage tracing studies suggest that SHP2 plays an important role in regulating the differentiation of terminal hypertrophic chondrocytes into osteoblasts, primarily affecting the metaphyseal trabecular bone formation; it has minimal effect on cortical bone.

SHP2 deletion in COL10 α 1-expressing hypertrophic chondrocytes promotes chondrocytic but represses osteogenic gene expression. After establishing that SHP2 influences the osteogenic differentiation of hypertrophic chondrocytes, we next investigated SHP2-related changes in gene and protein expression. To do so, we examined the effect of SHP2 deletion on osteogenic and chondrogenic marker expression in Col10 α 1-expressing chondrocytes using *in situ* hybridization and immunohistochemistry. We found that Col2 α 1 was upregulated in the metaphyseal region of the tibias from P1.5 SHP2_{Col10 α 1}KO;R26^{mTG} mice compared to SHP2_{Col10 α 1}CTR;R26^{mTG} controls, and that the osteogenic genes *Ibsp*, *Mmp13*, *Runx2*, and *Ctmb1* were all down-regulated (Fig. 5). Staining of sections from P1.5 newborns revealed that SOX9 protein was significantly increased in the hypertrophic chondrocytes of SHP2_{Col10 α 1}KO mice (Fig. 6A, red bar; Fig. S9), and that the transcript for *Sox9* was increased in the upper hypertrophic chondrocytes (Fig. 6B). Both *Sox9* and SOX9 were expressed in similar quantities in the physal proliferating chondrocytes in the SHP2_{Col10 α 1}CTR and SHP2_{Col10 α 1}KO mice (Fig. 6A,B). Immunostaining for β -CATENIN was non-informative as the protein levels were sufficiently low that they were beyond detection.

To corroborate our *in situ* and immunostaining data, we sought further validation of the regulation of SOX9 and chondrocyte gene expression by SHP2 *in vitro*. We were forced to use proliferating rather than hypertrophic chondrocytes for this signaling study due to the technical difficulty of obtaining homogenous populations of hypertrophic chondrocytes. To do so, we established ribcage chondrocyte cell lines that expressed either normal (SHP2^{WT}) or reduced (SHP2^{KD}) levels of SHP2 (via shRNA against murine SHP2) that could be induced (or not) to ablate SOX9 expression by tamoxifen administration (SOX9^{cKO} and SOX9^{WT}). Our nomenclature for the cell lines was SHP2^{WT}SOX9^{WT}, SHP2^{WT}SOX9^{cKO}, SHP2^{KD}SOX9^{WT}, and SHP2^{KD}SOX9^{cKO} for the wild type, SOX9 conditional knockout, SHP2 knockdown, and dual SHP2 knockdown/SOX9 conditional knockout, respectively

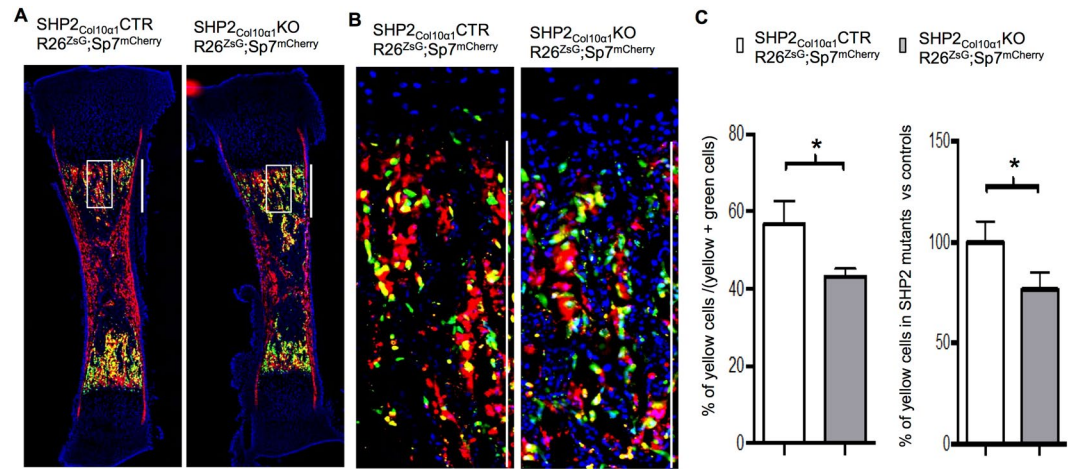


Figure 4. SHP2 deletion in COL10 α 1-expressing chondrocytes arrests their osteogenic differentiation. **(A)** Representative fluorescent images of mouse tibia sections demonstrating the abundance and distribution of COL10 α 1-expressing chondrocytes (ZsG⁺), OSTERIX⁺ osteoblasts (RFP⁺) and osteoblasts derived from COL10 α 1-expressing chondrocytes (ZsG⁺/RFP⁺, yellow) in P0.5-day-old SHP2^{Col10 α 1}CTR;R26^{ZsG};Sp7^{mCherry} mice ($n = 3$) and SHP2^{Col10 α 1}KO;R26^{ZsG};Sp7^{mCherry} mice ($n = 3$). **(B)** Enlarged views of the corresponding boxed areas in **A** demonstrating the reduction of ZsG⁺/RFP⁺ double positive (yellow) cells on trabecular bone surfaces in SHP2^{Col10 α 1}KO;R26^{ZsG};Sp7^{mCherry} mice, compared to SHP2^{Col10 α 1}CTR;R26^{ZsG};Sp7^{mCherry} controls ($n = 3$). The scale bar on the right is 500 μ m. Only cells within the 500 μ m \times 50 μ m rectangular region of interest were counted. **(C)** Bar graphs depicting the number of COL10 α 1⁺-cell-derived osteoblasts. SHP2 deletion in COL10 α 1-expressing chondrocytes compromised their osteogenic differentiation, compared to the controls ($n = 3$, * $p < 0.05$, Student's t test).

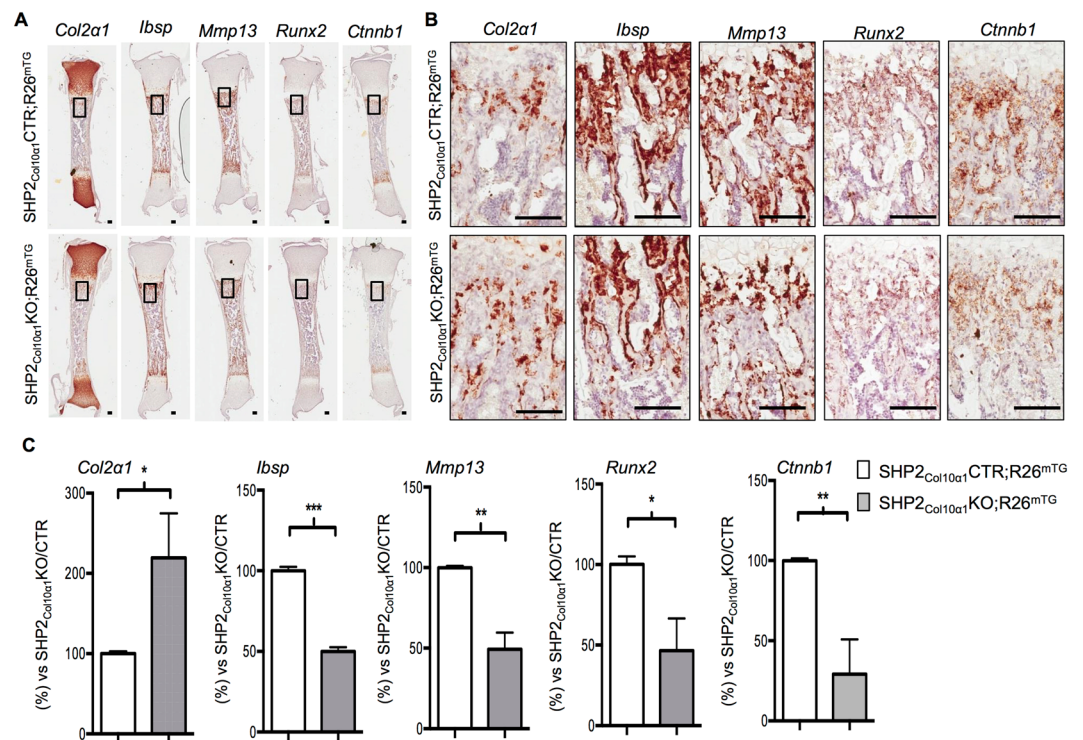


Figure 5. SHP2 deletion in COL10 α 1-expressing chondrocytes sustains the expression of chondrocytic but represses the expression of osteogenic genes. **(A)** Representative images of P0.5-day-old mouse tibia sections hybridized *in situ* with the probes indicated to assess the abundance of gene transcripts. **(B)** Enlarged views of corresponding boxed areas in **A**. **(C)** Bar graphs demonstrating an increase of *Col2a1* and a decrease of *Ibsp*, *Mmp13*, *Runx2* and *Ctnnb1* in the SHP2^{Col10 α 1}KO; R26^{mTG} mice, compared to the controls ($n = 3$, * $p < 0.05$, ** $p < 0.01$, and *** $p < 0.001$, Student's t test.). Scale bar: 100 μ m.

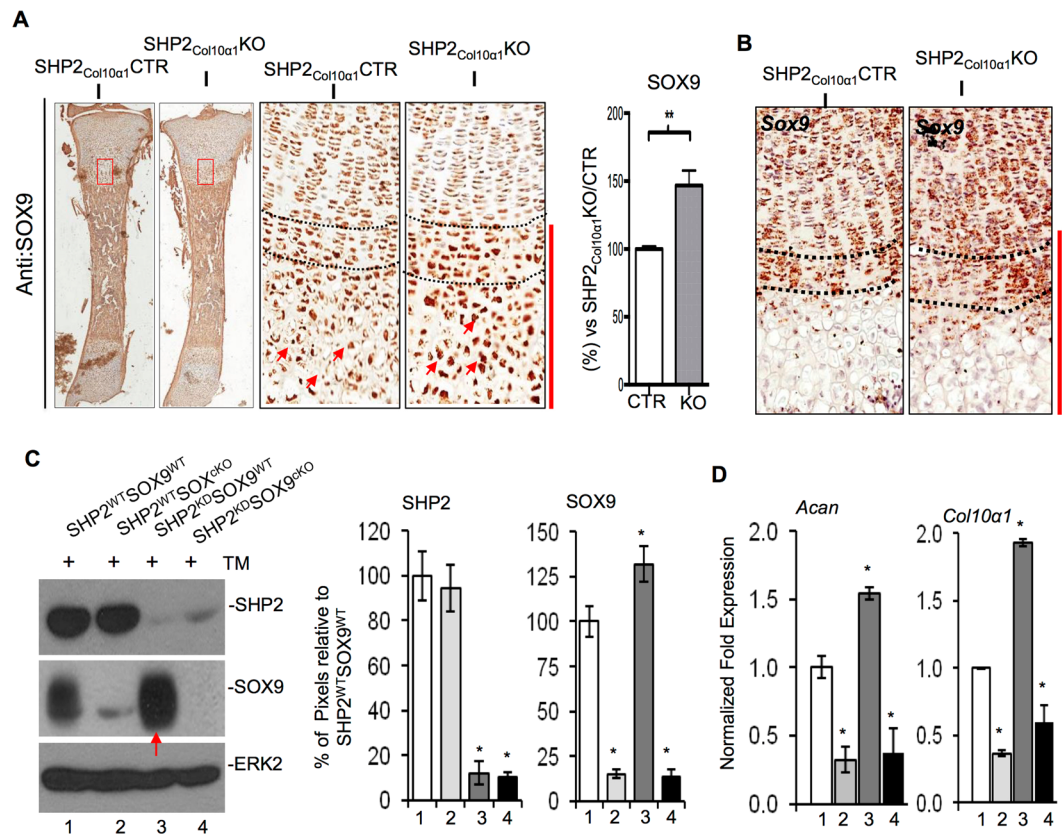


Figure 6. SHP2 deletion in hypertrophic chondrocytes increases SOX9 abundance and reducing *Sox9* in hypertrophic chondrocytes restores osteogenic gene expression in SHP2^{Col10α1}KO mice. **(A)** Representative images of P1.5 mouse tibia sections immunostained with SOX9 antibody (left), with enlarged views of the boxed areas (middle). Quantification of SOX9 expression in hypertrophic chondrocytes is shown on the right. SOX9 expression was elevated in the hypertrophic chondrocytes of SHP2^{Col10α1}KO (KO) mice, compared to SHP2^{Col10α1}CTR (CTR). (n = 3, **p < 0.01, Student's *t* test). **(B)** Images of the proximal tibia sections demonstrating the abundance of *Sox9* in P0.5 SHP2^{Col10α1}CTR and SHP2^{Col10α1}KO mice. *In situ* hybridization was carried out using RNAscope technology. Transcript abundance was visualized by DAB staining of HRP-conjugated DNA probes. Note that the height of the hypertrophic zone was increased in SHP2^{Col10α1}KO mice, accompanied by an expansion of the *Sox9*-expressing top layer (between dotted lines) of the hypertrophic zone. Expression of *Sox9* and SOX9 was comparable in proliferating chondrocytes between SHP2^{Col10α1}CTR and SHP2^{Col10α1}KO mice, n = 3. **(C)** Western blots (left) and bar graphs (right) demonstrating the expression of SHP2 and SOX9 in immortalized SHP2^{WT}SOX9^{WT}, SHP2^{WT}SOX9^{cKO}, SHP2^{KD}SOX9^{WT} and SHP2^{KD}SOX9^{cKO} chondrocytes (See Supplementary Fig. 10 for the full-length blots). SHP2 was efficiently knocked down in SHP2^{KD}SOX9^{WT} and SHP2^{KD}SOX9^{cKO} chondrocytes, and SOX9 was robustly deleted in SHP2^{WT}SOX9^{cKO} and SHP2^{KD}SOX9^{cKO} chondrocytes with tamoxifen treatment. Importantly, SHP2 knockdown in SHP2^{KD}SOX9^{WT} cells significantly increases the level of SOX9. Note that SHP2 was markedly knocked down in SHP2^{KD}SOX9^{WT} and SHP2^{KD}SOX9^{cKO} chondrocytes and SOX9 was robustly deleted in SHP2^{WT}SOX9^{cKO} and SHP2^{KD}SOX9^{cKO} chondrocytes upon TM treatment. Importantly SHP2 knockdown in SHP2^{KD}SOX9^{WT} chondrocytes significantly increased SOX9 abundance (red arrow) (*p < 0.05, Student's *t* test; n = 3). **(D)** qRT-PCR data show the increased transcript abundance of chondrocytic genes *Acan* and *Col10α1* in SHP2^{KD}SOX9^{WT} chondrocytes in which SOX9 was upregulated upon SHP2 knockdown. SHP2^{WT}SOX9^{WT} chondrocytes served as controls. Note that the elevated abundance of *Acan* and *Col10α1* in SHP2^{KD}SOX9^{WT} chondrocytes was rescued by SOX9 deletion in SHP2^{KD}SOX9^{cKO} chondrocytes (n = 3, *p < 0.05, Student's *t* test).

(Fig. S7A,B). SOX9 knockout was effected by 96 hours of exposure to 4-OH tamoxifen (TM) to induce *Sox9* deletion, and total cell lysates were analyzed by western blotting and total RNA was used for qRT-PCR.

SOX9 was robustly deleted upon TM treatment and SHP2 was effectively knocked down by the shRNA (Figs 6C; S10). As anticipated, the transcript level for the chondrocytic genes *Acan* and *Col10α1* decreased significantly in the tamoxifen-mediated SOX9 deleted SHP2^{KD}SOX9^{cKO} and SHP2^{WT}SOX9^{cKO} chondrocytes (Fig. 6D). Importantly, the abundance of both SOX9 and the transcripts for the chondrocytic genes *Acan* and *Col10α1* increased significantly in the SHP2^{KD}SOX9^{WT} chondrocytes compared to the SHP2^{WT}SOX9^{WT} controls (Fig. 6C,D), providing compelling evidence that SHP2 modifies *Acan* and *Col10α1* expression via SOX9. Similar results were also obtained on E17.5 embryos in which SHP2 was deleted in COL2α1-expressing cells (Fig. S6).

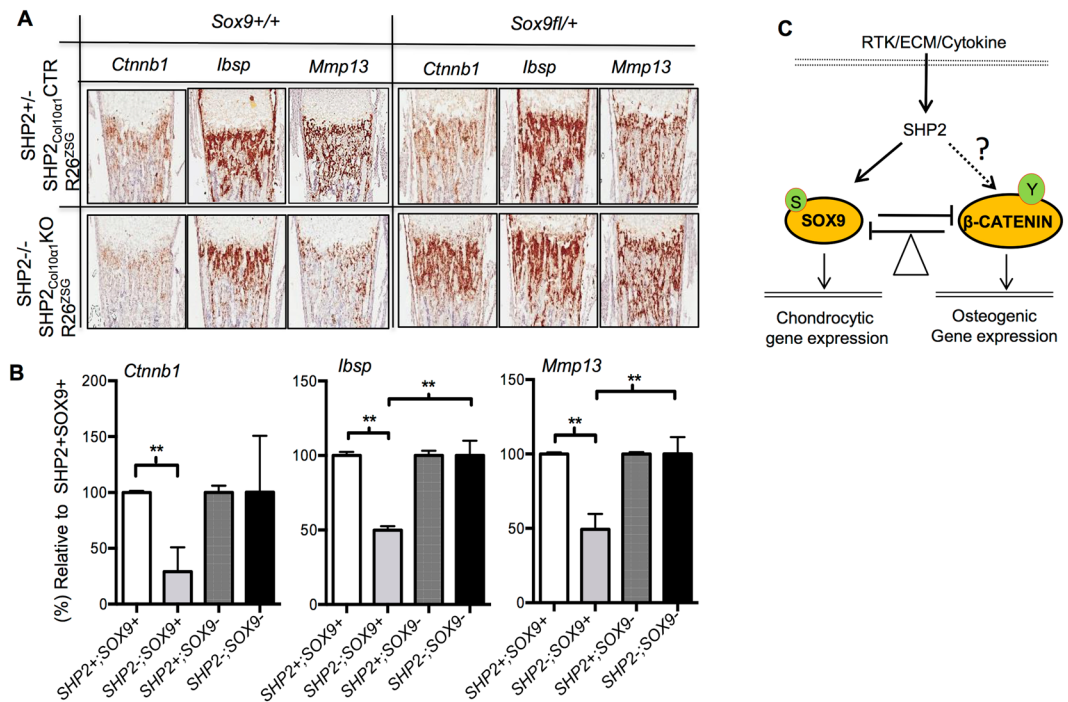


Figure 7. Haploinsufficiency of *Sox9* in SHP2 deficient hypertrophic chondrocytes restores osteogenic marker gene expression. **(A)** Representative images of P1.5 mouse tibia frozen sections hybridized *in situ* to the probes indicated demonstrating the abundance of *Ctnnb1*, *Ibsp*, and *Mmp13*. The expression of *Ctnnb1*, *Ibsp*, and *Mmp13* was reduced in SHP2^{Col10α1}KO;Sox9^{+/+} (SHP2–SOX9⁺) mice, compared to SHP2^{Col10α1}CTR;Sox9^{+/+} (SHP2+SOX9⁺) controls. Removal of one allele of *Sox9* from the hypertrophic chondrocytes in SHP2^{Col10α1}KO;Sox9^{+/–} mice (SHP2–SOX9[–]) restored the expression of *Ctnnb1*, *Ibsp*, and *Mmp13* comparable to SHP2+SOX9⁺ controls. **(B)** *In situ* hybridization data quantified using NIH ImageJ. n = 3, **p < 0.01, Student's t test. **(C)** Diagram depicting the working model by which SHP2 modifies the signals evoked by receptor tyrosine kinases (RTK), extracellular matrix proteins (ECM) and cytokines, and the expression of SOX9 and β-CATENIN. Tilting the expression of SOX9 and β-CATENIN in the hypertrophic chondrocytes due to SHP2 deletion favors chondrogenic but represses osteogenic differentiation. S:Serine, Y:Tyrosine.

Taken together, our cell lineage tracing and *in situ* hybridization studies suggest that SHP2 influences osteoblastogenesis and endochondral ossification, at least in part, by promoting the differentiation of hypertrophic chondrocytes into osteoblasts, and that SHP2 modulates the osteogenic differentiation of hypertrophic chondrocytes by indirectly influencing the expression and activity of osteogenic transcription factors via SOX9.

Haploinsufficiency of *Sox9* rescues the osteogenic differentiation of hypertrophic chondrocytes in SHP2^{Col10α1}KO mice. To confirm our finding that SHP2 acts through SOX9 to modulate the osteogenic differentiation of hypertrophic chondrocytes, we carried out a genetic rescue experiment in which *Sox9* haploinsufficiency would offset the chondrogenic effect of SHP2 deletion. *Sox9* wild type (*Sox9*^{+/+}) and heterozygous *Sox9* floxed mice (*Sox9*^{fl/+}) were crossed to SHP2^{Col10α1}CTR;R26^{ZsG} and SHP2^{Col10α1}KO;R26^{ZsG} mice, to yield mice in which both SHP2 and *Sox9* were modulated in Col10α1-expressing cells. Characterization of the mice in which *Sox9* was halved in the hypertrophic chondrocytes demonstrated that the transcript levels for the osteogenic genes *Ctnnb1*, *Ibsp* and *Mmp13*, were significantly increased (*in situ* hybridization and quantification using NIH ImageJ), as were the number of GFP+ cells in the metaphyseal cancellous bone (Fig. S8). Presumably these GFP+ cells are osteoblasts that had transdifferentiated from hypertrophic chondrocytes labeled with the R26^{ZsG} reporter. Lineage tracing using tibias from P0.5 newborns showed that loss of one allele of *Sox9* did not significantly affect the number of ZsGreen+ cells (Fig. S8A top) or/and the abundance of osteogenic gene transcripts, *Ctnnb1*, *Ibsp*, and *Mmp13* (Fig. S8B top) in the metaphyseal cancellous bone of the SHP2^{Col10α1}CTR;SOX9^{fl/+};R26^{ZsG} mice compared to SHP2^{Col10α1}CTR;SOX9^{+/+};R26^{ZsG} controls. In contrast, both the number of ZsGreen+ cells (Fig. S8 bottom) and the abundance of osteogenic marker genes markedly increased in the corresponding regions of the SHP2^{Col10α1}KO;SOX9^{fl/+};R26^{ZsG} mice, compared to SHP2^{Col10α1}KO;SOX9^{+/+};R26^{ZsG} controls (Fig. 7B, bottom, S8 bottom). Collectively these data provide convincing evidence that SHP2 regulates osteogenic differentiation in the primary spongiosa, a process that has been shown to include transdifferentiation of hypertrophic chondrocytes. Importantly, they also show that this regulation is mediated in part by SOX9.

Discussion

SHP2 is ubiquitously expressed, but little is known about its function in the skeletal system. Recently SHP2 loss-of-function mutations have been linked to the cartilage tumor syndrome metachondromatosis^{35–38} and scoliosis³⁷, suggesting a crucial role for SHP2 in the skeleton. To further study the role of SHP2 in cartilage, we adopted a genetic loss of function approach and ablated SHP2 expression in COL2 α 1⁺ (proliferating) and COL10 α 1⁺ (hypertrophic) chondrocytes respectively in mice. Phenotypic characterization showed that mice lacking SHP2 in the hypertrophic chondrocytes appeared normal through 10 weeks of age with the exception of a slight decrease in bone mineral density. In contrast, mice deficient SHP2 in the proliferating chondrocytes had a drastic skeletal phenotype. Developmental SHP2 deletion in COL2 α 1⁺ chondrocytes caused midgestation lethality (around E11.5), but postnatal SHP2 deletion in the same cell population led to scoliosis, expansion of the growth plate cartilage affecting both proliferating and hypertrophic chondrocytes, chondrodysplasia, enchondromas, exostoses, and reduced bone mineral density. These findings are consistent with published work showing the formation of scoliosis and enchondroma-like lesions on the vertebrae of SHP2^{COL2 α 1ER}KO mice and altered chondrocyte maturation and disorganized vertebral growth plates^{37,50}. The distinct bone and cartilage phenotypes in the mice lacking SHP2 in proliferating and hypertrophic chondrocytes suggest that SHP2 has a developmental stage-specific role in chondrogenesis and bone mineral homeostasis and that the cellular signaling networks wired in the proliferating and hypertrophic chondrocytes are complex.

It's not surprising that SHP2 deletion in COL2 α 1-expressing cells during development caused embryonic lethality in mice. It's well known that SHP2 is essential for early embryogenesis and for multiple organs/tissues development^{53,54}; *Col2 α 1* promoter is reportedly active not only in chondroid cells, but also in the mesenchyme of the frontal nasal mass, spinal neural tube, and the most ventral and dorsal parts of the forebrain during early embryogenesis^{61–63}. The midgestation lethality of SHP2^{COL2 α 1}KO mice and the survival of mice with postnatal SHP2 deletion in the COL2 α 1-expressing cells suggest that the lethality likely resulted from SHP2 deletion in COL2 α 1⁺ non-chondroid cells.

Although the transdifferentiation of hypertrophic chondrocytes into osteoblasts^{8–10} and their involvement in endochondral ossification and mineral homeostasis have been reported^{49,59}, the molecular mechanism(s) that regulates this process remains incompletely understood. Our data suggest that SHP2 is a key regulator for the osteogenic differentiation of hypertrophic chondrocytes. Mice deficient in SHP2 in COL10 α 1⁺ chondrocytes had a reduction of bone mineral density, BV/TV and Tb.Th, and an increased layer of hypertrophic chondrocytes within the growth plate. Indeed, our cell lineage tracing studies revealed that SHP2 deletion in COL10 α 1⁺ chondrocytes significantly decreased the number of osteoblasts marked by both *Col10 α 1-Cre;R26ZsG* and *Sp7^{mCherry}* dual reporters in the cancellous bone region, which was accompanied by a reduction of osteogenic marker gene transcripts *Ibsp*, *Runx2* and *Ctnnb1*. Collectively these data indicate that SHP2 is a key regulator for the differentiation of hypertrophic chondrocytes into osteoblasts.

Commitment of condensed mesenchymal cells into chondrocytes and osteoblasts requires several fate decisions, which are modified by multiple signaling pathways and transcription factors, including SOX9 and β -CATENIN^{39–42}. SOX9 is one of the earliest makers for mesenchymal condensation and for the commitment of mesenchymal progenitors to osteochondroprogenitors⁴³. With the progression of skeletal development, SOX9 is mainly restricted to the epiphyseal proliferating chondrocytes, maintains chondrocyte columnar proliferation^{41,43} and drives cell hypertrophy⁴². Although SOX9 persists after *Sox9* expression ceases in the hypertrophic chondrocytes in the growth plate, it was reported that *Sox9* is expressed in the upper layer of the COL10 α 1⁺ hypertrophic zone⁴². In hypertrophic chondrocytes, SOX9 keeps β -CATENIN in check and inhibits osteoblastic differentiation⁴². Conversely β -CATENIN promotes the osteogenic commitment of osteochondroprogenitors^{39,52,64} and hypertrophic chondrocytes; deletion of β -CATENIN in COL10 α 1⁺ cells impairs trabecular bone formation^{49,59,65}. Importantly, SOX9 and β -CATENIN reciprocally regulate one another in an antagonistic manner. Disrupting the balance of SOX9 and β -CATENIN signaling in skeletal cells modifies the chondrogenic or osteogenic fate decision^{45,66,67}.

We examined the effect of SHP2 deletion in COL10⁺ chondrocytes via the expression of SOX9, β -CATENIN, *Sox9* and *Ctnnb1*. Although β -CATENIN and *Ctnnb1* were below the level of detection in these cells, SOX9 and *Sox9* was significantly upregulated in the hypertrophic zone and in the upper layer of the hypertrophic zone, respectively. Given that β -CATENIN signaling is essential for the osteogenic differentiation of hypertrophic chondrocytes and the reciprocally antagonistic regulatory relationship of β -CATENIN and SOX9, we therefore proposed a model (Fig. 7C) wherein SHP2 regulates the osteogenic differentiation of hypertrophic chondrocytes by balancing SOX9 and β -CATENIN signaling. This model is supported by the results of our rescue experiment, where removal of one allele of *Sox9* in the SHP2 deficient hypertrophic chondrocytes restored the expression of osteogenic marker genes *Ctnnb1* and *Ibsp*. However, this experiment didn't exclude the possibility that the increase of SOX9 is due to the reduction of β -CATENIN as the consequence of SHP2 deletion in COL10 α 1⁺ chondrocytes. Indeed, SHP2 is reported to regulate the tyrosyl phosphorylation of β -CATENIN and its stability in other types of cells⁶⁸. The work of evaluating how SHP2 regulates the expression of SOX9 and β -CATENIN in chondrocytes is ongoing in our laboratory.

The distinct skeletal phenotypes in mice lacking SHP2 in the COL2 α 1- and COL10 α 1-expressing cells suggest that SHP2 has a development-stage-specific effect in chondrogenesis. Proliferating and hypertrophic chondrocytes are distinct in several aspects. First, the proliferation potential of chondrocytes markedly declines when they gradually transition from the proliferating to the hypertrophic stage. And second, this morphological switch is accompanied by the qualitative and quantitative change of gene expression profiles, which affect certain ligands^{69,70}, receptors^{71,72}, extracellular matrix proteins and transcription factors. Some of them or their downstream effectors may serve as the target of SHP2^{36,66,73}. This may explain why the phenotypic outcomes are different in mice with SHP2 ablation in the COL2 α 1- and COL10 α 1-expressing cells^{73–75}.

The etiology of enchondromas and exostoses, common benign cartilaginous lesions, remain elusive. Anatomically, exostoses and enchondromas arise adjacent to the growth plate cartilage and resemble it morphologically. This suggests that growth plate chondrocytes may be candidate cells-of-origin and that dysregulation of cellular signaling pathways that modulate growth plate chondrocytes could contribute to the pathogenesis of these lesions⁷⁶. The findings from this study support these views. Mice with SHP2 deletion in COL2 α 1⁺ chondrocytes grew exostoses and enchondromas at the metaphysis of the long bones, affecting hip, tibia, phalanges and vertebrae; chondrocytes with SHP2 knockout or knockdown had an elevated cell proliferation and chondrocytic gene expression. Most importantly, SHP2 knockout or knockdown in chondrocytes *in vivo* and *in vitro* significantly increases the expression of SOX9, a master chondrogenic transcription factor^{43,77} that has also been shown as the driving force of tumorigenesis in multiple organs and tissues^{78–80}. Our results and published work indicate that SHP2 normally represses the proliferation and/or maturation of chondrocytes, functioning as a tumor suppressor in cartilage. However, SHP2 is historically considered as an oncogene and essential for the development and/or homeostasis of multiple organs and tissues^{28,29}. The double-edged sword effect of SHP2 (tumorigenic and anti-tumorigenic) in different types of cells reflects the complexity of cellular signaling networks and the particular “wiring” of the signaling pathways therein.

In sum, we found that SHP2 regulates the differentiation of hypertrophic chondrocytes to an osteoblastic fate, a transition that is critical for endochondral bone formation, bone mineral and cartilage homeostasis. Our study also illustrates an important role for SHP2 in the embryonic and postnatal cartilage development. Its effect on osteogenesis is mediated by SOX9-mediated β -CATENIN signaling. Therefore, manipulating SHP2 and SHP2-regulated signaling pathways can potentially facilitate the development of novel therapeutics to treat cartilage and bone developmental and degenerative diseases.

Methods

Animals. *Ptpn11* floxed (*Ptpn11*^{fl/+})³⁶, *Sox9* floxed (*Sox9*^{fl/+})^{41,81}, *Tg(Col2 α 1-Cre)*⁵⁷, *Tg(Col2 α 1-CreER^{T2})*⁵⁵, *Tg(Col10 α 1-Cre)*⁵⁶, *Tg(CMV-CreER^{T2})*⁸², *Tg(Sp7/mCherry)* (*Sp7*^{mCherry})⁶⁰, *Rosa26^{lacZ}* (*R26^{lacZ}*)⁵⁸, *Rosa26^{ZsG}* (*R26^{ZsG}*)⁸³ and *Rosa26^{mTmG}* (*R26^{mTmG}*)⁸⁴ mice were reported previously. PCR genotyping conditions for *Ptpn11*^{fl} and *Sox9*^{fl} alleles, *R26^{lacZ}* and *R26^{mTmG}* reporters and Cre transgenes have been described in the original publications and are available upon request. To delete SHP2 in chondrocytes that express collagen type II, alpha-1 (COL2 α 1) and type X, alpha-1 (COL10 α 1), a *Ptpn11* floxed allele was interbred to *Tg(Col2 α 1-Cre)*, *Tg(Col2 α 1-CreER^{T2})* and *Tg(Col10 α 1-Cre)* mice to generate offspring with the following nomenclature: SHP2_{Col2 α 1}CTR, SHP2_{Col2 α 1}KO, SHP2_{Col2 α 1ER}CTR, SHP2_{Col2 α 1ER}KO, SHP2_{Col10 α 1}CTR, and SHP2_{Col10 α 1}KO, respectively (Fig. S1A,B). To delete SOX9 in chondrocytes *in vitro*, a *Sox9* floxed allele was interbred to *Tg(CMV-CreER^{T2})* mice to generate *Sox9*^{fl/fl} and *Sox9*^{fl/fl}; *Tg(CMV-CreER^{T2})* offspring, abbreviated respectively as SOX9^{WT} and SOX9^{CKO} mice (Fig. S7). To trace COL2 α 1 and COL10 α 1-expressing cells *in vivo*, SHP2_{Col2 α 1ER}CTR, SHP2_{Col2 α 1ER}KO, SHP2_{Col10 α 1}CTR and SHP2_{Col10 α 1}KO mice were also bred with *R26^{lacZ}* or *R26^{mTmG}* reporters, respectively. *R26^{mTmG}* reporter expresses fluorescent protein Tomato Red ubiquitously before Cre recombination and GFP following recombination. To induce *Tg(Col2 α 1-CreER)* activity, 4-OH tamoxifen (TM; Sigma, MO) was dissolved in DMSO-ethanol-corn oil (4:6:90) mixture at a concentration of 10 mg/mL and injected intraperitoneally into SHP2_{Col2 α 1ER}CTR, SHP2_{Col2 α 1ER}KO mice (1 mg/per mouse/each dose)^{55,85}. All transgenic mice were maintained on C57BL/6J background.

Control and SHP2 mutant animals were sacrificed at the indicated time points and used for x-ray, histological, biochemical and biological analyses. All animal work was reviewed and approved by the Rhode Island Hospital Institutional Animal Care and Use Committee (Assurance No. A3922-01) and performed in accordance with PHS policy on the humane care and use of laboratory animals.

Chondrocyte isolation and cultures. Primary chondrocytes were derived from 1- to 3-day-old pups with modified procedures⁸⁶. Briefly, the ventral parts of the rib cages from newborn mice were collected and incubated with trypsin-EDTA (0.25%, Invitrogen) for 1 hour at 37 °C. After washing with PBS, the rib cages were further incubated with hyaluronidase (2 mg/ml; Sigma) for 2 hours and hyaluronidase/collagenase D mixture (1 mg/ml, Roche) for 4 hours in DMEM at 37 °C. Undigested bony tissues were discarded by filtration, chondrocytes were collected by centrifugation and cultured in DMEM/F12 medium (1:1) (Invitrogen) supplemented with 10% of FBS, and 1% of ampicillin and streptomycin.

To immortalize primary chondrocytes, retrovirus expressing SV40 large T antigen were prepared from 293 T cells^{36,87} and used to infect chondrocytes (passage 1) overnight in the presence of 4 μ g/ml polybrene. Infected cells were cultured for 48 hours and then selected with neomycin for 7 days. Neomycin-resistant clones were pooled, expanded, and used for this study. To knock down SHP2 expression in SOX9^{WT} and SOX9^{CKO} chondrocytes, retrovirus expressing a control (SHP2^{WT}) or short hairpin RNAi against murine SHP2 (SHP2^{KD}) were prepared and used to infect SOX9^{WT} and SOX9^{CKO} chondrocytes as described previously^{36,88}. Puromycin-resistant chondrocytes were selected, expanded and used for this study. To induce SOX9 deletion *in vitro*, SOX9^{WT} and SOX9^{CKO} chondrocytes were exposed to TM (1 μ M) in the culture medium for 72 hours⁵⁰. TM-treated chondrocytes were then used for biological and biochemical studies.

Antibodies and Reagents. Polyclonal antibodies against murine SHP2 and SOX9 were purchased from Santa Cruz and EMD Millipore, respectively. Monoclonal antibody against murine ERK2 was purchased from Santa Cruz. Alcian blue and Safranin O staining solutions were purchased from Poly Scientific.

Histology analysis and von Kossa staining. Femurs and tibias from control and SHP2 mutant mice were fixed in 4% formaldehyde for 3 days, decalcified, paraffin-embedded, and sectioned to stain with hematoxylin and eosin (H&E), alcian blue and Safranin O /fast green. To trace the fate of COL2 α 1- and COL10 α 1-expressing chondrocytes *in vivo*, femurs and tibias were collected from SHP2_{Col2 α 1ER}CTR; *R26^{mTmG}*, SHP2_{Col2 α 1ER}KO; *R26^{mTmG}*,

SHP2^{Col10α1}CTR;R26^{mTG} and SHP2^{Col10α1}KO;R26^{mTG} mice at the indicated time points and fixed in 4% formaldehyde overnight. Frozen sections were examined microscopically to visualize green (GFP) and red (RFP) fluorescent protein-positive cells. DAPI was used for nucleus counterstaining. All fluorescent and phase contrast images were taken using a Nikon digital fluorescence microscope and Aperio slide scanner (Vista, CA). Immunostaining was carried out using Vectorstain ImmPACT/DAB kit following the manufacturer's instruction. von Kossa staining was carried out using commercially-available kits, per the manufacturer's instructions (Millipore).

In situ hybridization. Femurs and tibias were collected from neonates at the indicated time points, fixed in 4% formaldehyde overnight, and then embedded in OCT compound. 10 μm frozen sections were cut using a cryostat for *in situ* hybridization with probes against murine *Sox9*, *Acan*, *Col2α1*, *Col1α1*, *Ctnnb1*, *Ibsp*, *Runx2* and *Mmp13*. Hybridization and detection of hybridization signals were achieved using RNAscope HD-Brown kit per the manufacturer's instruction (Advanced Cell Diagnostics).

Quantitative RT-PCR analyses. Total RNA was extracted from chondrocytes using RNeasy kit (Qiagen). cDNA was synthesized using 1 μg of total RNA with iScriptTM cDNA Synthesis Kit (Bio-Rad) and qRT-PCR was performed with RT²SYBR[®] Green kit on a Bio-Rad CFX machine. All samples were normalized to *Gapdh* and *Actin*; gene expression was presented as fold increases or decreases compared with that of controls. All primer sequences used for this study are listed in the Supplementary Table 1.

μ-CT and X-ray radiograph analysis. X-ray imaging analysis of mice skeletons was done immediately after euthanasia using a digital radiography system (MX-20, Faxitron Bioptics, LLC, Tucson, AZ, USA). High resolution 3D volume images were generated using a desktop μ-CT40 system (Scanco Medical AG, CH) after fixation of bone specimens in 4% formaldehyde.

Western blot analysis. Cells were lysed into modified NP-40 lysis buffer (0.5% NP40, 150 mM NaCl, 1 mM EDTA, 50 mM Tris [pH 7.4]) supplemented with a protease inhibitor cocktail (1 mM PMSE, 10 mg/ml aprotinin, 0.5 mg/ml antipain, and 0.5 mg/ml pepstatin)⁵³. For immunoblotting, cell lysates (30–50 μg) were resolved by SDS-PAGE, transferred to PVDF membranes, and incubated with primary antibodies for 2 hours or overnight at 4 °C (according to the manufacturer's instructions), followed by incubation with HRP-conjugated secondary antibodies (Bio-Rad).

Statistical analysis. Statistical differences between groups were evaluated by student *t* and χ^2 tests. A *p* value of <0.05 was considered to be significant. Analyses were performed by using Prism 3.0 (GraphPad, San Diego, CA) and Excel (Microsoft).

References

- Nakashima, K. & de Crombrughe, B. Transcriptional mechanisms in osteoblast differentiation and bone formation. *Trends Genet* **19**, 458–466 (2003).
- Long, F. & Ornitz, D. M. Development of the endochondral skeleton. *Cold Spring Harb Perspect Biol* **5**, a008334, <https://doi.org/10.1101/cshperspect.a008334> (2013).
- de Crombrughe, B. *et al.* Transcriptional mechanisms of chondrocyte differentiation. *Matrix Biol* **19**, 389–394, doi:S0945-053X(00)00094-9 [pii] (2000).
- Olsen, B. R., Reginato, A. M. & Wang, W. Bone development. *Annu Rev Cell Dev Biol* **16**, 191–220, doi:10.1146/annurev.cellbio.16.1.191 [pii] (2000).
- Kronenberg, H. M. Developmental regulation of the growth plate. *Nature* **423**, 332–336, doi:10.1038/nature01657 nature01657 [pii] (2003).
- Bianco, P., Cancedda, F. D., Riminucci, M. & Cancedda, R. Bone formation via cartilage models: the “borderline” chondrocyte. *Matrix Biol* **17**, 185–192 (1998).
- Shapiro, I. M., Adams, C. S., Freeman, T. & Srinivas, V. Fate of the hypertrophic chondrocyte: microenvironmental perspectives on apoptosis and survival in the epiphyseal growth plate. *Birth Defects Res C Embryo Today* **75**, 330–339, <https://doi.org/10.1002/bdrc.20057> (2005).
- Ono, N., Ono, W., Nagasawa, T. & Kronenberg, H. M. A subset of chondrogenic cells provides early mesenchymal progenitors in growing bones. *Nat Cell Biol* **16**, 1157–1167, <https://doi.org/10.1038/ncb3067> (2014).
- Yang, L., Tsang, K. Y., Tang, H. C., Chan, D. & Cheah, K. S. Hypertrophic chondrocytes can become osteoblasts and osteocytes in endochondral bone formation. *Proc Natl Acad Sci USA* **111**, 12097–12102, <https://doi.org/10.1073/pnas.1302703111> (2014).
- Zhou, X. *et al.* Chondrocytes transdifferentiate into osteoblasts in endochondral bone during development, postnatal growth and fracture healing in mice. *PLoS Genet* **10**, e1004820, <https://doi.org/10.1371/journal.pgen.1004820> (2014).
- Nishimura, R. *et al.* Regulation of endochondral ossification by transcription factors. *Frontiers in bioscience (Landmark edition)* **17**, 2657–2666 (2012).
- Mackie, E. J., Ahmed, Y. A., Tatarczuch, L., Chen, K. S. & Mirams, M. Endochondral ossification: how cartilage is converted into bone in the developing skeleton. *Int J Biochem Cell Biol* **40**, 46–62, <https://doi.org/10.1016/j.biocel.2007.06.009> (2008).
- Golding, M. B., Tsuchimochi, K. & Ijiri, K. The control of chondrogenesis. *J Cell Biochem* **97**, 33–44, <https://doi.org/10.1002/jcb.20652> (2006).
- Zuscik, M. J., Hilton, M. J., Zhang, X., Chen, D. & O'Keefe, R. J. Regulation of chondrogenesis and chondrocyte differentiation by stress. *J Clin Invest* **118**, 429–438, <https://doi.org/10.1172/JCI34174> (2008).
- Uusitalo, H., Hiltunen, A., Soderstrom, M., Aro, H. T. & Vuorio, E. Expression of cathepsins B, H, K, L, and S and matrix metalloproteinases 9 and 13 during chondrocyte hypertrophy and endochondral ossification in mouse fracture callus. *Calcified tissue international* **67**, 382–390 (2000).
- Stickens, D. *et al.* Altered endochondral bone development in matrix metalloproteinase 13-deficient mice. *Development* **131**, 5883–5895, <https://doi.org/10.1242/dev.01461> (2004).
- Zhou, Z. *et al.* Impaired endochondral ossification and angiogenesis in mice deficient in membrane-type matrix metalloproteinase I. *Proc Natl Acad Sci USA* **97**, 4052–4057, <https://doi.org/10.1073/pnas.060037197> (2000).
- Nakashima, T. *et al.* Evidence for osteocyte regulation of bone homeostasis through RANKL expression. *Nat Med* **17**, 1231–1234, <https://doi.org/10.1038/nm.2452> (2011).
- Xiong, J. *et al.* Matrix-embedded cells control osteoclast formation. *Nat Med* **17**, 1235–1241, <https://doi.org/10.1038/nm.2448> (2011).

20. Naski, M. C., Colvin, J. S., Coffin, J. D. & Ornitz, D. M. Repression of hedgehog signaling and BMP4 expression in growth plate cartilage by fibroblast growth factor receptor 3. *Development* **125**, 4977–4988 (1998).
21. Ornitz, D. M. FGF signaling in the developing endochondral skeleton. *Cytokine Growth Factor Rev* **16**, 205–213, <https://doi.org/10.1016/j.cytogfr.2005.02.003> (2005).
22. Liu, J. P., Baker, J., Perkins, A. S., Robertson, E. J. & Efstratiadis, A. Mice carrying null mutations of the genes encoding insulin-like growth factor I (Igf-1) and type 1 IGF receptor (Igf1r). *Cell* **75**, 59–72, doi:0092-8674(93)90679-K [pii] (1993).
23. Wang, J., Zhou, J. & Bondy, C. A. Igf1 promotes longitudinal bone growth by insulin-like actions augmenting chondrocyte hypertrophy. *FASEB J* **13**, 1985–1990 (1999).
24. Ehlen, H. W., Buelens, L. A. & Vortkamp, A. Hedgehog signaling in skeletal development. *Birth Defects Res C Embryo Today* **78**, 267–279, <https://doi.org/10.1002/bdrc.20076> (2006).
25. Yoon, B. S. *et al.* Bmpr1a and Bmpr1b have overlapping functions and are essential for chondrogenesis *in vivo*. *Proc Natl Acad Sci USA* **102**, 5062–5067, doi:0500031102 [pii] 10.1073/pnas.0500031102 (2005).
26. Day, T. F. & Yang, Y. Wnt and hedgehog signaling pathways in bone development. *J Bone Joint Surg Am* **90**(Suppl 1), 19–24, <https://doi.org/10.2106/jbjs.g.01174> (2008).
27. Baron, R., Rawadi, G. & Roman-Roman, S. Wnt signaling: a key regulator of bone mass. *Curr Top Dev Biol* **76**, 103–127, [https://doi.org/10.1016/s0070-2153\(06\)76004-5](https://doi.org/10.1016/s0070-2153(06)76004-5) (2006).
28. Grossmann, K. S., Rosario, M., Birchmeier, C. & Birchmeier, W. The tyrosine phosphatase Shp2 in development and cancer. *Adv Cancer Res* **106**, 53–89, doi:S0065-230X(10)06002-1 [pii] 10.1016/S0065-230X(10)06002-1 (2010).
29. Neel, B. G., Chan G., Dhanji S. SH2 Domain-Containing Protein-Tyrosine Phosphatases. *Handbook of Cell Signaling*, 771–809 (2009).
30. Kosaki, K. *et al.* PTPN11 (protein-tyrosine phosphatase, nonreceptor-type 11) mutations in seven Japanese patients with Noonan syndrome. *J Clin Endocrinol Metab* **87**, 3529–3533 (2002).
31. Tartaglia, M. *et al.* Mutations in PTPN11, encoding the protein tyrosine phosphatase SHP-2, cause Noonan syndrome. *Nat Genet* **29**, 465–468 (2001).
32. Araki, T. *et al.* Mouse model of Noonan syndrome reveals cell type- and gene dosage-dependent effects of Ptpn11 mutation. *Nat Med* **10**, 849–857, <https://doi.org/10.1038/nm1084> (2004).
33. Nakamura, T., Gulick, J., Pratt, R. & Robbins, J. Noonan syndrome is associated with enhanced pERK activity, the repression of which can prevent craniofacial malformations. *Proc Natl Acad Sci USA* **106**, 15436–15441, doi:0903302106 [pii]10.1073/pnas.0903302106 (2009).
34. Nakamura, T. *et al.* Mediating ERK 1/2 signaling rescues congenital heart defects in a mouse model of Noonan syndrome. *J Clin Invest* **117**, 2123–2132, <https://doi.org/10.1172/JCI30756> (2007).
35. Bowen, M. E. *et al.* Loss-of-function mutations in PTPN11 cause metachondromatosis, but not Ollier disease or Maffucci syndrome. *PLoS Genet* **7**, e1002050, <https://doi.org/10.1371/journal.pgen.1002050> (2011).
36. Yang, W. *et al.* Ptpn11 deletion in a novel progenitor causes metachondromatosis by inducing hedgehog signalling. *Nature* **499**, 491–495, <https://doi.org/10.1038/nature12396> (2013).
37. Kim, H. K. *et al.* Induction of SHP2-deficiency in chondrocytes causes severe scoliosis and kyphosis in mice. *Spine*, doi:<https://doi.org/10.1097/BRS.0b013e3182a3d370> (2013).
38. Sobreira, N. L. *et al.* Whole-genome sequencing of a single proband together with linkage analysis identifies a Mendelian disease gene. *PLoS Genet* **6**, e1000991, <https://doi.org/10.1371/journal.pgen.1000991> (2010).
39. Day, T. F., Guo, X., Garrett-Beal, L. & Yang, Y. Wnt/beta-catenin signaling in mesenchymal progenitors controls osteoblast and chondrocyte differentiation during vertebrate skeletogenesis. *Dev Cell* **8**, 739–750, <https://doi.org/10.1016/j.devcel.2005.03.016> (2005).
40. Harley, V. & Lefebvre, V. Twenty Sox, twenty years. *Int J Biochem Cell Biol* **42**, 376–377, <https://doi.org/10.1016/j.biocel.2009.12.004> (2010).
41. Akiyama, H., Chaboissier, M. C., Martin, J. F., Schedl, A. & de Crombrugge, B. The transcription factor Sox9 has essential roles in successive steps of the chondrocyte differentiation pathway and is required for expression of Sox5 and Sox6. *Genes Dev* **16**, 2813–2828, <https://doi.org/10.1101/gad.1017802> (2002).
42. Dy, P. *et al.* Sox9 directs hypertrophic maturation and blocks osteoblast differentiation of growth plate chondrocytes. *Dev Cell* **22**, 597–609, <https://doi.org/10.1016/j.devcel.2011.12.024> (2012).
43. Bi, W., Deng, J. M., Zhang, Z., Behringer, R. R. & de Crombrugge, B. Sox9 is required for cartilage formation. *Nat Genet* **22**, 85–89, <https://doi.org/10.1038/8792> (1999).
44. Hattori, T. *et al.* SOX9 is a major negative regulator of cartilage vascularization, bone marrow formation and endochondral ossification. *Development* **137**, 901–911, <https://doi.org/10.1242/dev.045203> (2010).
45. Akiyama, H. *et al.* Interactions between Sox9 and beta-catenin control chondrocyte differentiation. *Genes Dev* **18**, 1072–1087, doi:<https://doi.org/10.1101/gad.117110418/9/1072> [pii] (2004).
46. Lefebvre, V., Behringer, R. R. & de Crombrugge, B. L-Sox5, Sox6 and Sox9 control essential steps of the chondrocyte differentiation pathway. *Osteoarthritis Cartilage* **9**(Suppl A), S69–75 (2001).
47. Zorn, A. M. *et al.* Regulation of Wnt signaling by Sox proteins: XSox17 alpha/beta and XSox3 physically interact with beta-catenin. *Mol Cell* **4**, 487–498 (1999).
48. Kormish, J. D., Sinner, D. & Zorn, A. M. Interactions between SOX factors and Wnt/beta-catenin signaling in development and disease. *Dev Dyn* **239**, 56–68, <https://doi.org/10.1002/dvdy.22046> (2010).
49. Houben, A. *et al.* beta-catenin activity in late hypertrophic chondrocytes locally orchestrates osteoblastogenesis and osteoclastogenesis. *Development*, doi:<https://doi.org/10.1242/dev.137489> (2016).
50. Bowen, M. E., Ayturk, U. M., Kurek, K. C., Yang, W. & Warman, M. L. SHP2 Regulates Chondrocyte Terminal Differentiation, Growth Plate Architecture and Skeletal Cell Fates. *PLoS Genet* **10**, e1004364, <https://doi.org/10.1371/journal.pgen.1004364> (2014).
51. Lapinski, P. E., Meyer, M. F., Feng, G. S., Kamiya, N. & King, P. D. Deletion of SHP-2 in mesenchymal stem cells causes growth retardation, limb and chest deformity and calvarial defects in mice. *Dis Model Mech* **6**, 1448–1458, <https://doi.org/10.1242/dmm.012849> (2013).
52. Hill, T. P., Spater, D., Taketo, M. M., Birchmeier, W. & Hartmann, C. Canonical Wnt/beta-catenin signaling prevents osteoblasts from differentiating into chondrocytes. *Dev Cell* **8**, 727–738, <https://doi.org/10.1016/j.devcel.2005.02.013> (2005).
53. Yang, W. *et al.* An Shp2/SFK/Ras/Erk signaling pathway controls trophoblast stem cell survival. *Dev Cell* **10**, 317–327, <https://doi.org/10.1016/j.devcel.2006.01.002> (2006).
54. Saxton, T. *et al.* Abnormal mesoderm patterning in mouse embryos mutant for the SH2 tyrosine phosphatase Shp-2. *EMBO J* **16**, p2352–2364 (1997).
55. Zhu, M., Chen, M., Lichtler, A. C., O’Keefe, R. J. & Chen, D. Tamoxifen-inducible Cre-recombination in articular chondrocytes of adult Col2a1-CreER(T2) transgenic mice. *Osteoarthritis Cartilage* **16**, 129–130, doi:S1063-4584(07)00279-8 [pii]10.1016/j.joca.2007.08.001 (2008).
56. Gebhard, S. *et al.* Specific expression of Cre recombinase in hypertrophic cartilage under the control of a BAC-Col10a1 promoter. *Matrix Biol* **27**, 693–699, doi:S0945-053X(08)00104-2 [pii]10.1016/j.matbio.2008.07.001 (2008).

57. Ovchinnikov, D. A., Deng, J. M., Ogunrinu, G. & Behringer, R. R. Col2a1-directed expression of Cre recombinase in differentiating chondrocytes in transgenic mice. *Genesis* **26**, 145–146, doi:10.1002/(SICI)1526-968X(200002)26:2<145::AID-GENE14>3.0.CO;2-C [pii] (2000).
58. Soriano, P. Generalized lacZ expression with the ROSA26 Cre reporter strain. *Nat Genet* **21**, 70–71, <https://doi.org/10.1038/5007> (1999).
59. Golovchenko, S. *et al.* Deletion of beta catenin in hypertrophic growth plate chondrocytes impairs trabecular bone formation. *Bone* **55**, 102–112, <https://doi.org/10.1016/j.bone.2013.03.019> (2013).
60. Strecker, S., Fu, Y., Liu, Y. & Maye, P. Generation and characterization of Osterix-Cherry reporter mice. *Genesis* **51**, 246–258, <https://doi.org/10.1002/dvg.22360> (2013).
61. Cheah, K. S., Lau, E. T., Au, P. K. & Tam, P. P. Expression of the mouse alpha 1(II) collagen gene is not restricted to cartilage during development. *Development* **111**, 945–953 (1991).
62. Wood, A., Ashhurst, D. E., Corbett, A. & Thorogood, P. The transient expression of type II collagen at tissue interfaces during mammalian craniofacial development. *Development* **111**, 955–968 (1991).
63. Aszodi, A., Chan, D., Hunziker, E., Bateman, J. F. & Fassler, R. Collagen II is essential for the removal of the notochord and the formation of intervertebral discs. *J Cell Biol* **143**, 1399–1412 (1998).
64. Hill, T. P., Taketo, M. M., Birchmeier, W. & Hartmann, C. Multiple roles of mesenchymal beta-catenin during murine limb patterning. *Development* **133**, 1219–1229, <https://doi.org/10.1242/dev.02298> (2006).
65. Park, J. *et al.* Dual pathways to endochondral osteoblasts: a novel chondrocyte-derived osteoprogenitor cell identified in hypertrophic cartilage. *Biol Open* **4**, 608–621, <https://doi.org/10.1242/bio.201411031> (2015).
66. Shung, C. Y., Ota, S., Zhou, Z. Q., Keene, D. R. & Hurlin, P. J. Disruption of a Sox9-beta-catenin circuit by mutant Fgfr3 in thanatophoric dysplasia type II. *Hum Mol Genet* **21**, 4628–4644, <https://doi.org/10.1093/hmg/dd3305> (2012).
67. Topol, L., Chen, W., Song, H., Day, T. F. & Yang, Y. Sox9 inhibits Wnt signaling by promoting beta-catenin phosphorylation in the nucleus. *J Biol Chem* **284**, 3323–3333, <https://doi.org/10.1074/jbc.M808048200> (2009).
68. Timmerman, I. *et al.* The tyrosine phosphatase SHP2 regulates recovery of endothelial adherens junctions through control of beta-catenin phosphorylation. *Mol Biol Cell* **23**, 4212–4225, <https://doi.org/10.1091/mbc.E12-01-0038> (2012).
69. Haigh, J. J., Gerber, H. P., Ferrara, N. & Wagner, E. F. Conditional inactivation of VEGF-A in areas of collagen2a1 expression results in embryonic lethality in the heterozygous state. *Development* **127**, 1445–1453 (2000).
70. Kiepe, D., Ciarmatori, S., Haarmann, A. & Tonshoff, B. Differential expression of IGF system components in proliferating vs. differentiating growth plate chondrocytes: the functional role of IGFBP-5. *Am J Physiol Endocrinol Metab* **290**, E363–371, doi:00363.2005 [pii] 10.1152/ajpendo.00363.2005 (2006).
71. Karolak, M. R., Yang, X. & Eleferiou, F. FGFR1 signaling in hypertrophic chondrocytes is attenuated by the Ras-GAP neurofibromin during endochondral bone formation. *Hum Mol Genet* **24**, 2552–2564, <https://doi.org/10.1093/hmg/ddv019> (2015).
72. Iwata, T. *et al.* A neonatal lethal mutation in FGFR3 uncouples proliferation and differentiation of growth plate chondrocytes in embryos. *Hum Mol Genet* **9**, 1603–1613 (2000).
73. Ahmed, Z. *et al.* Grb2 controls phosphorylation of FGFR2 by inhibiting receptor kinase and Shp2 phosphatase activity. *J Cell Biol* **200**, 493–504, <https://doi.org/10.1083/jcb.201204106> (2013).
74. Leung, V. Y. *et al.* SOX9 governs differentiation stage-specific gene expression in growth plate chondrocytes via direct concomitant transactivation and repression. *PLoS Genet* **7**, e1002356, <https://doi.org/10.1371/journal.pgen.1002356> (2011).
75. Hart, K. C. *et al.* Transformation and Stat activation by derivatives of FGFR1, FGFR3, and FGFR4. *Oncogene* **19**, 3309–3320 (2000).
76. Bovee, J. V., Hogendoorn, P. C., Wunder, J. S. & Alman, B. A. Cartilage tumours and bone development: molecular pathology and possible therapeutic targets. *Nat Rev Cancer* **10**, 481–488, doi:nrc2869 [pii] 10.1038/nrc2869 (2010).
77. Akiyama, H. Control of chondrogenesis by the transcription factor Sox9. *Modern rheumatology/the Japan Rheumatism Association* **18**, 213–219, <https://doi.org/10.1007/s10165-008-0048-x> (2008).
78. Larsimont, J. C. *et al.* Sox9 Controls Self-Renewal of Oncogene Targeted Cells and Links Tumor Initiation and Invasion. *Cell Stem Cell* **17**, 60–73, <https://doi.org/10.1016/j.stem.2015.05.008> (2015).
79. Matheu, A. *et al.* Oncogenicity of the developmental transcription factor Sox9. *Cancer Res* **72**, 1301–1315, <https://doi.org/10.1158/0008-5472.CAN-11-3660> (2012).
80. Pritchett, J., Athwal, V., Roberts, N., Hanley, N. A. & Hanley, K. P. Understanding the role of SOX9 in acquired diseases: lessons from development. *Trends Mol Med* **17**, 166–174, <https://doi.org/10.1016/j.molmed.2010.12.001> (2011).
81. Kist, R., Schrewe, H., Balling, R. & Scherer, G. Conditional inactivation of Sox9: a mouse model for campomelic dysplasia. *Genesis* **32**, 121–123 (2002).
82. Hayashi, S. & McMahon, A. P. Efficient recombination in diverse tissues by a tamoxifen-inducible form of Cre: a tool for temporally regulated gene activation/inactivation in the mouse. *Dev Biol* **244**, 305–318, <https://doi.org/10.1006/dbio.2002.0597> (2002).
83. Madisen, L. *et al.* A robust and high-throughput Cre reporting and characterization system for the whole mouse brain. *Nature neuroscience* **13**, 133–140, <https://doi.org/10.1038/nn.2467> (2010).
84. Muzumdar, M. D., Tasic, B., Miyamichi, K., Li, L. & Luo, L. A global double-fluorescent Cre reporter mouse. *Genesis* **45**, 593–605, <https://doi.org/10.1002/dvg.20335> (2007).
85. Chen, M. *et al.* Generation of a transgenic mouse model with chondrocyte-specific and tamoxifen-inducible expression of Cre recombinase. *Genesis* **45**, 44–50, <https://doi.org/10.1002/dvg.20261> (2007).
86. Lefebvre, V. *et al.* Characterization of primary cultures of chondrocytes from type II collagen/beta-galactosidase transgenic mice. *Matrix Biol* **14**, 329–335 (1994).
87. Hahn, W. C. *et al.* Enumeration of the simian virus 40 early region elements necessary for human cell transformation. *Mol Cell Biol* **22**, 2111–2123 (2002).
88. Hidaka, K. *et al.* Involvement of the phosphoinositide 3-kinase/protein kinase B signaling pathway in insulin/IGF-I-induced chondrogenesis of the mouse embryonal carcinoma-derived cell line ATDC5. *Int J Biochem Cell Biol* **33**, 1094–1103, doi:S1357-2725(01)00067-X [pii] (2001).

Acknowledgements

We would like to thank Scott McAllister and Paul Monfils for X-ray radiographs and histology analysis. This publication was made possible by the NIGMS Grant #8P20GM103468 and NIAMS Grant RO1AR066746 (to W.Y.). This work was also supported by the Rhode Island Hospital Orthopaedic Foundation and a grant from Arthritis National Research Foundation (W.Y.).

Author Contributions

L.W., C.Z., J.H., D.M. and W.Y. contributed to data collection; J.H. and Q.W. carried out histological staining and data interpretation; L.X. conducted μ CT data collection and analysis; K.V.D.M., D.C. and X.Y. provided key reagents for this study; M.G.E. and M.L.W. contributed important intellectual content; D.A.M. and W.Y. wrote the manuscript. All authors read and approve the final version of this manuscript.

Additional Information

Supplementary information accompanies this paper at <https://doi.org/10.1038/s41598-017-12767-9>.

Competing Interests: The authors declare that they have no competing interests.

Publisher's note: Springer Nature remains neutral with regard to jurisdictional claims in published maps and institutional affiliations.



Open Access This article is licensed under a Creative Commons Attribution 4.0 International License, which permits use, sharing, adaptation, distribution and reproduction in any medium or format, as long as you give appropriate credit to the original author(s) and the source, provide a link to the Creative Commons license, and indicate if changes were made. The images or other third party material in this article are included in the article's Creative Commons license, unless indicated otherwise in a credit line to the material. If material is not included in the article's Creative Commons license and your intended use is not permitted by statutory regulation or exceeds the permitted use, you will need to obtain permission directly from the copyright holder. To view a copy of this license, visit <http://creativecommons.org/licenses/by/4.0/>.

© The Author(s) 2017